Int. J. Electrochem. Sci., 8 **(2013)** 3371 - 3378

International Journal of
ELECTROCHEMICAL
SCIENCE
www.electrochemsci.org

Short Communication

Porous Tin Oxide Nanoplatelets as Excellent-Efficiency Photoelectrodes and Gas Sensors

Yi-Zhou Zhang[1,2], *Huan Pang*[2,*], *Yanqiu Sun*[3], *Wen-Yong Lai*[*,1], *Ang Wei*[1], *Wei Huang*[*,1]

[1] Key Laboratory for Organic Electronics & Information Displays (KLOEID), Institute of Adanced Materials (IAM), Nanjing University of Posts and Telecommunications (NUPT), Nanjing 210046, China
[2] College of Chemistry and Chemical Engineering, Anyang Normal University, Anyang, 455000, Henan, P. R. China.
[3] College of nano science & technology, Soochow University, Suzhou, 215006, Jiangsu, P. R. China.
[*]E-mail: iamwylai@njupt.edu.cn; iamwhuang@njupt.edu.cn; huanpangchem@hotmail.com

Received: 26 January 2013 / *Accepted:* 15 February 2013 / *Published:* 1 March 2013

Porous SnO_2 nanoplatelets are successfully synthesized by calcinations of SnS_2 nanoplatelets. Interestingly, the measurement of dye-sensitized solar cells shows that porous SnO_2 nanoplatelets is a good candidate of photoelectrode materials in dye-sensitized solar cells with large improvement in photoconversion efficiency. More importantly, the as-prepared porous SnO_2 nanoplatelets also exhibit good gas-sensing properties to ethanol.

Keywords: Porous SnO_2 nanoplatelets; Dye-sensitized solar cells; Gas-sensing

1. INTRODUCTION

Recently, many efforts have been devoting to synthesize various micro-nanostructures, such as nanodots, nanorods, nanowires, nanoplates, nanospheres and three-dimensional ordered superstructures, due to their interesting properties of such micro-nanostructures and their potential applications in lots of fields [1-6], including catalysis [7], optoelectronics [8], lithium-ion batteries [9], drug delivery system [10], sensors [11, 12] and antibacterial agent [13, 14].However, methods to manipulation of these ordered structural materials have often need surfactants [15-17], copolymers [18, 19], and porous alumina as templates. Patterned-metal-catalyzed routes have also been used [20-22]. However, the main drawback of these methods is the need for complete template removal, otherwise impurities will exist in the final products [23-27]. Controlled solution-growth synthesis routes for the growth of inorganic materials are attractive because of the simplicity of the synthesis process. Therefore, there is significant interest in developing spontaneous generation of novel patterns with tailored structures and shapes by facile, hard template-free, solution-based, morphology controlled approaches to building novel self-generated micro-nanostructures.

Tin oxide (SnO_2), an *n*-type semiconductor with a wide band gap (E_g = 3.6 eV, 300 K), is a promising candidate for the future generation of cost-effective photovoltaic solar cells in the field of dye-sensitized solar cells (DSSCs). [28–32] SnO_2 possesses remarkable receptivity variation in gaseous environment and excellent chemical stability, and is widely used in chemical sensors, dye-sensitized solar cells and transparent conductors. [33, 34] Because SnO_2 has a lower isoelectric point (iep, at pH 4–5) than anatase TiO_2 (iep at pH 6–7), which leads to less adsorption of the dye with acidic carboxyl groups (for example, $(Bu_4N)_2[Ru(Hdcbpy)_2(NCS)_2]$ (N719)), [35] SnO_2-based DSSCs were developed with less success, and the conversion efficiencies of SnO_2 photoelectrodes reported so far are much lower than those of TiO_2 in the past decade. [36, 37]

Recently, besides SnO_2-based film sensors, many SnO_2 nanostructured materials are used as gas sensors by researchers. [38-41] The large surface area of SnO_2 nanomaterials is crucial for light harvesting and gas absorbing, thus porous SnO_2 nanomaterials hold great promise as photoelectrodes and gas sensors. However, to date, there are few reports about synthesis of porous SnO_2 nanomaterials and successful application in photoelectrodes or gas sensors.

In this article, we report an easy route to synthesize porous SnO_2 nanoplatelets. The measurement of DSSCs shows that porous SnO_2 nanoplatelets is a good candidate of photoelectrode materials in DSSCs with large improvement in photoconversion efficiency. The as-prepared porous SnO_2 nanoplatelets exhibited good gas-sensing properties to ethanol.

2. EXPERIMENT

2.1. Synthesis of SnS_2 nanoplatelets and porous SnO_2 nanoplatelets.

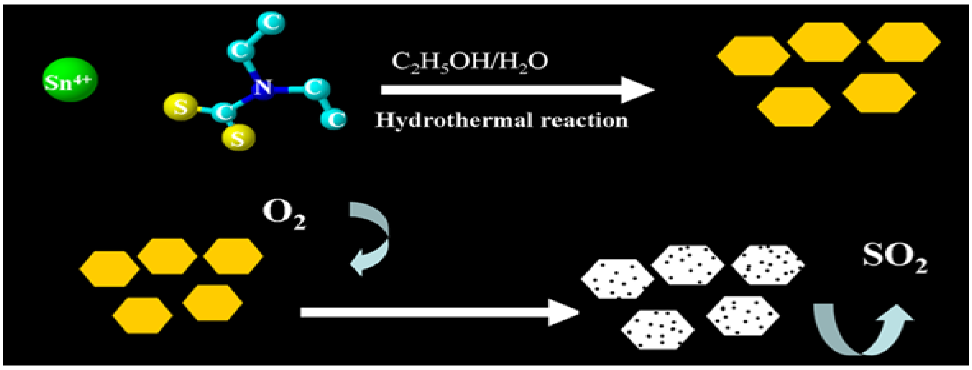

Scheme 1. A simple route of synthesis porous SnO_2 nanoplatelets.

All chemicals were analytical grade and used as received without further purification. Deionized water was used throughout. Scheme 1 shows the simple route of our work. Fisrtly, 0.2 g sodium diethyldithio carbarnate, 0.16 g $SnCl_4$, were mixed in 10 mL deionized water and 10 mL ethanol, then the solution was transferred into a 50 mL Teflon-lined stainless steel autoclave. The autoclave was sealed and maintained at 200 °C for 12 h. After the reaction was completed, the resulting products were filtered off, washed with absolute ethanol and distilled water several times, and then dried in the air; porous SnO_2 nanoplatelets can be obtained by calcining 0.05 g thus prepared SnS_2 nanoplatelets at 450 °C for 1 h in the air.

2.2. Characterization.

The morphology of the as-prepared samples was observed by a Hitachi S-4800 field-emission scanning electron microscope (FE-SEM) at an acceleration voltage of 10.0 kV. The phase analyses of the samples were performed by X-ray diffraction (XRD) on a SHIMADZU, XRD-6000 with Cu K_α radiation (λ = 1.5418 Å). Transmission electron microscopy (TEM) images, HRTEM image and the corresponding selected area electron diffraction (SAED) pattern were captured on the JEM-2100 instrument microscopy at an acceleration voltage of 200 kV.

2.3 Solar Cell Electrolyte.

The electrolyte solutions were freshly prepared immediately before each set of experiments as previously reported. [42] The electrolyte, 0.6 M 1,2-dimethyl-3-propylimidazolium iodide (made in house), 0.1 M LiI (Lancaster), 0.05 M I_2 (Lancaster), and 0.5 M 4-tert-butylpyridine (Aldrich) in acetonitrile, was introduced into the cell via a vacuum filling method.

2.4 Photoelectrochemistry.

The photoanode consisted of colloidal SnO_2 deposited upon an FTO substrate sensitized with either $Ru(deeb)(bpy)_2(PF_6)_2$, $Ru(deeb)_2(dpp)(PF_6)_2$, or $Ru(deeb)_2$-$(bpz)(PF_6)_2$. The counter electrode consisted of an FTO substrate with a thin Pt coating. Measurements were performed in a two electrode cell at room temperature using the I_3^-/I^-redox mediator, and at 0 °C for the $(SeCN)_2/SeCN^-$ and $(SCN)_2$/SCN redox mediators, with preparation methods discussed elsewhere. [42] A 150 W Xe lamp coupled to a *f*/2 0.2 m McPherson monochromator was used for incident photon-to-current efficiency (IPCE) measurements. The 488 nm laser line of an Innova argon ion laser was used as the excitation source for photocurrent density vs photovoltage and for irradiance-dependent measurements. Plasma lines were removed using a 488 nm notch filter, and the flux was attenuated using a beam collimator. Incident irradiances were measured using an S370 UDT optometer. Photocurrents and photovoltages were obtained using a Keithley 617 electrometer and a Keithley 199 System DMM/Scanner, respectively.

2.5. Structure and Preparation of the Sensor Device

The structures of the sensor device and the measurement system are the same as in the report. [43] The as-prepared porous SnO_2 nanoplatelets were directly coated on the outer surface of the ceramic tube and dried in air, then calcined at 350 °C for 3 h. The sensor response was defined as $S = R_{air}/R_{gas}$, where, R_{air} is the resistance in dry air and R_{gas} is that in the dry air mixed with detected gases.

3. RESULTS AND DISCUSSION

3.1. Structures and Morphologies of as-prepared SnS_2 nanoplatelets and porous SnO_2 nanoplatelets

XRD patterns in Figure 1a show the diffraction peaks of the as-prepared SnS_2 nanoplatelets (JCPDS-831705). The diffraction peaks are sharp enough, from which we can conclude that as-prepared SnS_2 nanoplatelets crystallize well.

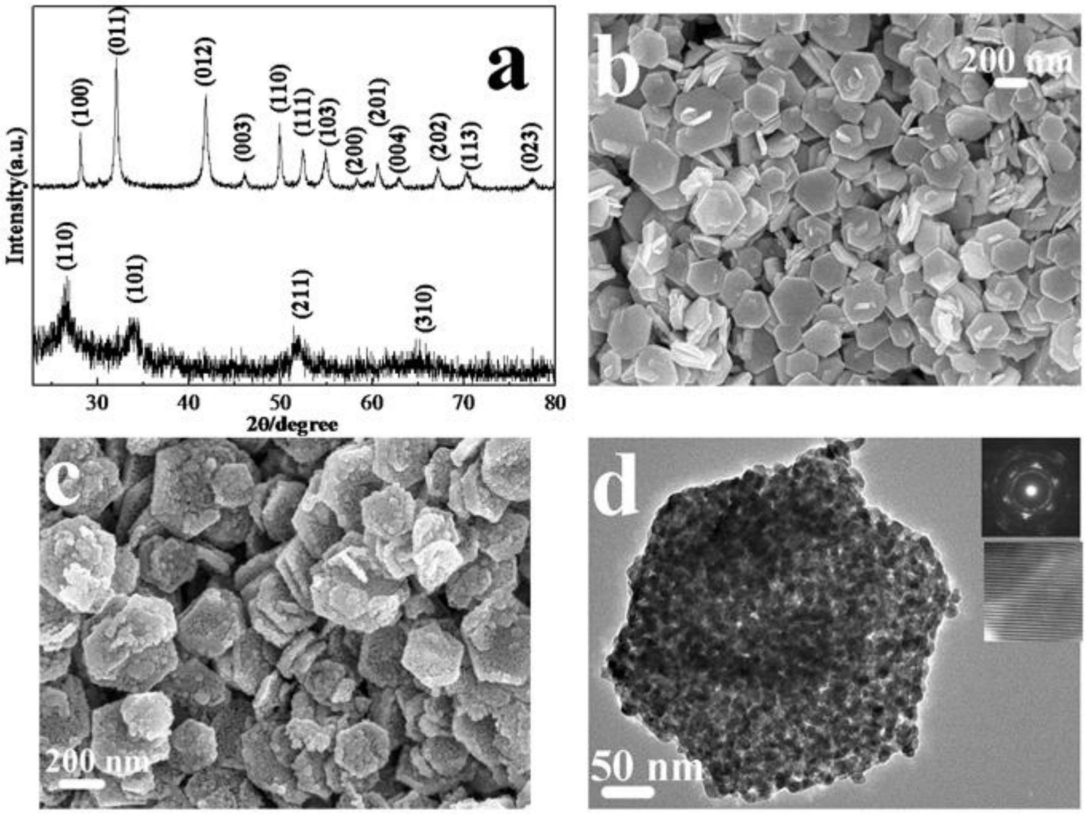

Figure 1. a) XRD patterns of SnS_2 nanoplatelets and SnO_2 porous nanoplatelets; b) SEM image of SnS_2; c) SEM of SnO_2 porous nanoplatelets, and d) Corresponding TEM images, (in inset of d SAED and HRTEM).

The diffraction peaks of SnO_2 (JCPDS 77-0450) turned wider after the removal the S atom by being calcined at 450 °C for 3 h in the air, which can be attributed to the small crystallite size of SnO_2

nanoparticles (JCPDS 77-0450). The morphologies of the samples are measured by FSEM, TEM (HRTEM). Figure 1b is the SEM image of the SnS_2 nanoplatelets, they are hexagon and have smooth surfaces. The width of each SnS_2 nanoplatelets is about 400-500 nm.

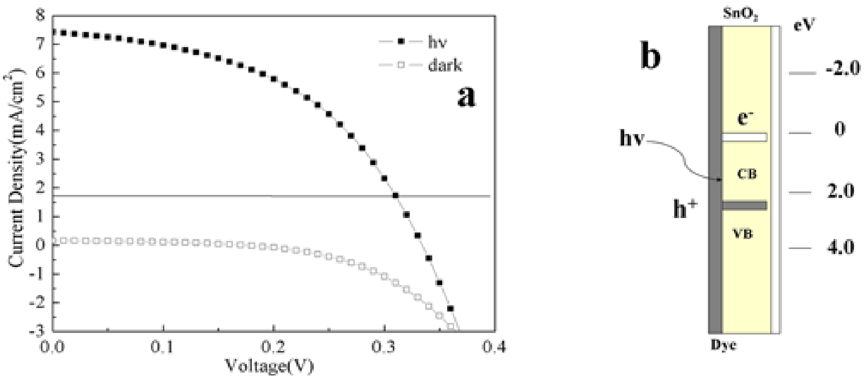

Figure 2. a) *I-V* characteristics of the DS made from porous SnO_2 nanoplatelets at an illumination intensity of 1000 Wm^{-2} 1.5 AM; b) Schematic diagram illustrating the energy levels of SnO_2 and excited energy levels of the Ru-dye.

After being calcined in the air, the SnS_2 nanoplatelets transform into porous SnO_2 nanoplatelets completely, which can be proved by the XRD pattern (Figure 1a). The porous SnO_2 nanoplatelets maintain the morphologies of the SnS_2 nanoplatelets well and have the same width as the SnS_2 nanoplatelets (Figure 1c). Unlike the SnS_2 nanoplatelets, the porous SnO_2 nanoplatelets have coarse surfaces. From Figure 1d, we can see that the porous SnO_2 nanoplatelets are composed of many SnO_2 nanocrystals. These nanocrystals do not felsite and form many mespores observed in the porous SnO_2 nanoplatelets. In the inset of Figure 1d are the corresponding SAED and HRTEM of the porous SnO_2 nanoplatelets (the Figure 1d), which show the polycrystalline nature of porous SnO_2 nanoplatelets and good crystallinity of each SnO_2 nanoparticle, in good consistency with XRD pattern (Figure 1a).

3.2 Dye-sensitized Solar Cells Measurement of the Porous SnO_2 Nanoplatelets

The CB and VB potentials of SnO_2 and excited levels of the Ru-dye are shown in Figure 3a. With the absorption of light, the electron in the dye excited level can be transferred to the CB of SnO_2. Once the electrons are transferred to the CB of SnO_2 from the excited dye, the electrons traverse effectively. The overall photoconversion efficiency (η) of the porous SnO_2 nanoplatelets DSSC is 3.5 %, remarkably about two times higher than those of SnO_2 multilayered hollow microspheres (η=1.4 %), and more than two times higher than those of nano-SnO_2 (η=1.0 %) DSSCs. [44] The improvement in η value of the porous SnO_2 nanoplatelets might be caused by the higher high surface area, leading to better adsorption of dye and increased light absorption by the porous SnO_2 nanoplatelets structure.

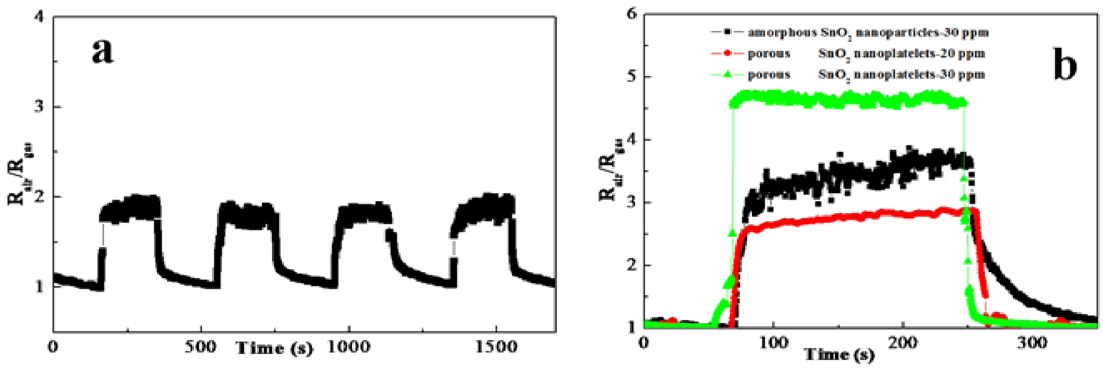

Figure 3. a) Resistance response of sensors based on porous SnO_2 nanoplatelets, the ethanol concentration in the ethanol–air mixture was at 10 ppm ethanol–air at 300 ^{o}C; b) Resistance response of sensors based on SnO_2 nanoparticles and porous SnO_2 nanoplatelets at 300℃.

3.3. Gas-Sensing Properties of the Porous SnO_2 Nanoplatelets

Figure 3 shows the ethanol sensing performance of the porous SnO_2 nanoplatelets. Ethanol gas sensing was measured in a close chamber, and the sensing test was performed at 300 ℃. Figure 3*a* shows the response and recovery characteristics of the porous SnO_2 nanoplatelets before and after being exposed to ethanol. R_{gas} and R_{air} are the resistance values of the sensors in mixed ethanol–air vapor and in air, respectively. The sensing properties are reproducible; the sensors show almost exactly the same response whether they are exposed to ethanol gas or not (Figure 3a). Figure 3b shows the sensing properties of our sample and SnO_2 nanoparticles commonly used in gas sensing, we can find that porous SnO_2 nanoplatelets have higher sensitivity; the value of R_{air} /R_{gas} of our sample obtained at 20 ppm ethanol gas is almost the same as the R_{air}/R_{gas} value obtained at 30 ppm ethanol gas for the commonly used SnO_2 nanoparticles. Beside, the response of the porous SnO_2 nanoplatelets is steady, which can be explained by the large absorption volume of SnO_2 nanoplatelets.

4. CONCLUSIONS

Porous and polycrystalline SnO_2 nanoplatelets were prepared by using SnS_2 nanoplatelets as a template. The porous SnO_2 nanoplatelets exhibit excellent photoconversion efficiency and high sensitivity and good reversibility toward ethanol gas. The good photoconversion efficiency and gas-sensing properties were attributed to the small size of SnO_2 nanoparticles and the porous microstructure of the SnO_2. This simple synthetic route to porous nanomaterials sheds light on the synthesis of many other metal oxides with similar structure.

ACKNOWLEDGMENT
This work was supported by the National Basic Research Program of China (973 Program, no. 2009CB930601), the National Natural Science Foundation of China (no. 20904024, 51173081， 61136003，61106036, 21201010), the Natural Science Foundation of Jiangsu Province (BK2011760), the Doctoral Fund of Ministry of Education of China (Grant 20093223120004), the NUPT Scientific Foundation (Grant NY210016, NY211124), and the Qing Lan Project of Jiangsu Province.

References

1. H. Pang, Y. Ma, G. Li, J. Chen, J. Zhang, H. Zheng and W. Du, *Dalton Trans.*, 41 (2012) 13284-13291.
2. H. Pang, Z. Yan, W. Wang, J. Chen, J. Zhang and H. Zheng, *Nanoscale*, 4 (2012) 5946-5953.
3. H. Pang, B. Zhang, J. Du, J. Chen, J. S. Zhang, S. Li, *RSC Adv*., 2 (2012) 2257
4. H. Pang, J. Deng, B. Yan, Y. Ma, G. Li, Y. Ai, J. Chen, J. Zhang, H. Zheng and J. Du, *Int. J. Electrochem. Sci.* 7 (2012) 10735-10747.
5. H. Pang, Z. Yan, W. Wang, Y. Wei, X. Li, J. Li, J. Chen, J. Zhang and H. Zheng, *Int. J. Electrochem. Sci.* 7 (2012) 12340-12353.
6. H. Pang, Z. Yan, Y. Ma, G. Li, J. Chen, J. Zhang, W. Du and S. Li, *J Solid State Electrochem* DOI 10.1007/s10008-013-2007-5
7. C. Burda, X. B. Chen, R. Narayanan, M. A. El-Sayed, *Chem. Rev.*, 105 (2005) 1025
8. X. Duan, Y. Huang, Y. Cui, J. Wang, C. M. Lieber, *Nature*, 409 (2001) 66
9. A. M. Cao, J. S. Hu, H. P. Liang, L. J. Wan, *Angew. Chem. Int. Ed.*, 44 (2005) 4391
10. Y. Cai, H. Pan, X. Xu, Q. Hu, L. Li, R. Tang, *Chem. Mater.*, 19 (2007) 3081
11. D. F. Zhang, L. D. Sun, G. Xu, C. H. Yan, *Phys. Chem. Chem. Phys.*, 8 (2006) 4874
12. F. Favier, E. C. Walter, M. P. Zach, T. Benter, R. M. Penner, *Science*, 293 (2001) 2227
13. T. Zhang, W. Dong, M. Keeter-Brewer, K. Sanjit, R. N. Njabon, Z. R. Tian, *J. Am. Chem. Soc.*, 128 (2006) 10960
14. S. H. Yu, M. Yoshimura, *Adv. Mater.*, 14 (2002) 296
15. L. Manna, D. J. Milliron, A. Meisei, E. C. Scher, A. P. Alivisatos, *Nat. Mater.*, 2 (2003) 382
16. Y. W. Jun, Y. Y. Jung, J. Cheon, *J. Am.Chem. Soc.*, 124 (2002) 615
17. T. K. Sau, C. J. Murphy, *J. Am. Chem. Soc.*, 126 (2004) 8648
18. S. H. Yu, H. Cölfen, M. Antonietti, *Chem. Eur. J.*, 8 (2002) 2937
19. L. Q. H. Cölfen, M. Antonietti, M. Li, J. D. Hopwood, A. J. Ashley, S. Mann, *Chem. Eur. J.*, 7 (2001) 3526
20. B. T. Holland, C. F. Blanford, A. Stein, *Science*, 281 (1998) 538
21. H. Cao, Y. Xu, J. Hong, H. Liu, G. Yin, B. Li, C. Tie, Z. Xu, *Adv. Mater.*, 13 (2001) 1393
22. T. Martensson, P. Carlberg, M. Borgström, L. Montelius, W. Seifert, L. Samuelson, *Nano Lett.*, 4 (2004) 699
23. R. Ma, Y. Bando, L. Zhang, T. Sasaki, *Adv. Mater.*, 16 (2004) 918
24. X. Wang, Y. Li, *Chem. Eur. J.*, 9 (2003) 300
25. X. Wang, Y. Li, *J. Am. Chem. Soc.*, 124 (2002) 2880
26. X. F. Shen, Y. S. Ding, J. Liu, J. Cai, K. Laubernds, R. P. Zerger, A. Vasiliev, M. Aindow, S. L. Suib, *Adv. Mater.*, 17 (2005) 805
27. P. Levy, A. G. Leyva, H. E. Troiani,d R. D. Sanchez, *Appl. Phys. Lett.*, 83 (2003) 5247.
28. B. O'Regan, M. Grätzel, *Nature*, 353 (1991) 737.
29. P. Wang, S. M. Zakeeruddin, J. E. Moser, M. K. Nazeeruddin, T. Sekiguchi,M. Grätzel, *Nat. Mater.*, 2 (2003) 402.
30. M. Grätzel, *Inorg. Chem.*, 44 (2005) 6841.
31. J. H. Wu, Z. Lan, J. M. Lin, M. L. Huang, S. C. Hao, T. Sato, S. Yin, *Adv.Mater.*, 19 (2007) 4006.
32. Y. Bai, Y. Cao, J. Zhang, M. Wang, R. Li, P. Wang, S. M. Zakeeruddin, M.Grätzel, *Nat. Mater.*, 7 (2008) 626.
33. Q. Kuang,C. S. Lao, Z. L. Wang, Z. X. Xie and L. S. Zheng, *J. Am. Chem.Soc.*, 129 (2007) 6070.
34. (a) Y. Wang, H. C. Zeng and J. Y. Lee, *Adv. Mater.*, 18 (2006) 645; (b) H. Kim and J. Cho, *J. Mater. Chem.*, 18 (2008) 771
35. A. Kay, M. Grätzel, *Chem. Mater.*, 14 (2002) 2930.
36. S. Chappel, A. Zaban, *Sol. Energy Mater. Sol. Cells*, 71 (2002) 141.
37. Y. Fukai, Y. Kondo, S.Mori, E. Suzuki, *Electrochem. Commun.*, 9 (2007) 1439.

38. N. Pinna, G. Neri, M. Antonietti, M. Niederberger, *Angew. Chem.,Int. Ed.*, 43 (2004) 4345.
39. A. Kolmakov, Y. X. Zhang, G. S. Cheng, M. Moskovits, *Adv.Mater.*, 15 (2003) 997.
40. M. Law, H. Kind, B. Messer, F. Kim, P. D. Yang, *Angew. Chem.,Int. Ed.*, 41 (2002) 2405.
41. E. Comini, G. Faglia, G. Sberveglieri, Z. W. Pan, Z. L. Wang, *Appl. Phys. Lett.* , 81 (2002) 1869.
42. (a) G. Oskam, B. V. Bergeron, G. J. Meyer, P. C. Searson, *J.Phys. Chem. B*, 105 (2001) 6867-6873.
43. Z. Guo, J. Y. Liu, Y. Jia, X. Chen, F. L. Meng, M. Q. Li, J. H. Liu, *Nanotechnology*, 19 (2008) 345704.
44. H. Pang, Z. Yan, Y. Wei, X. Li, J. Li, L. Zhang,J. Chen, J. Zhang and H. Zheng, *Part. Part. Syst. Charact.*10.1002/ppsc.201200147.